SIMULATION OF AIR BREAKDOWN MECHANISM USING DIFFERENT ELECTRODES

A PROJECT SUBMITTED IN PARTIAL FULFILLMENT
OF THE REQUIREMENT FOR THE DEGREE OF

Bachelor of Technology
in
Electrical Engineering

By

A Srikant

(Roll No.: 107EE030)

&

Shekhar Chandra Pradhan

(Roll No.: 107EE051)

Department of Electrical Engineering
National Institute of Technology, Rourkela
Odisha
2011

SIMULATION OF AIR BREAKDOWN MECHANISM USING DIFFERENT ELECTRODES

A PROJECT SUBMITTED IN PARTIAL FULFILLMENT
OF THE REQUIREMENT FOR THE DEGREE OF

Bachelor of Technology
in
Electrical Engineering

By

A Srikant

(Roll No.:107EE030)

&

Shekhar Chandra Pradhan

(Roll No.:107EE051)

Under the guidance of

Prof. Subrata Karmakar

Department of Electrical Engineering
National Institute of Technology, Rourkela
Odisha
2011

National Institute of Technology
Rourkela

CERTIFICATE

This is to certify that the thesis entitled, "**SIMULATION OF AIR BREAKDOWN MECHANISM USING DIFFERENT ELECTRODES**" submitted by A Srikant and Shekhar Chandra Pradhan in partial fulfillment of the requirements for the award of Bachelor of Technology Degree in Electrical Engineering at the National Institute of Technology, Rourkela (Deemed University) is an authentic work carried out by them under my supervision and guidance.

To the best of my knowledge, the matter embodied in the thesis has not been submitted to any other university / institute for the award of any Degree or Diploma.

Date:

Prof. Subrata Karmakar
Dept. of Electrical Engineering
National Institute of Technology, Rourkela
Rourkela-769008

Acknowledgement

The research work related to this thesis has been carried out at High Voltage Laboratory, Department of Electrical Engineering, National Institute of Technology (NIT), Rourkela. This work would have been impossible without the help and guidance of several people, whose contribution we would like to acknowledge.

First of all, we would like to express our sincere and profound gratitude to our supervisor Dr. S. Karmakar, Professor of Electrical Engineering Department of National Institute of Technology Rourkela, for his consistent encouragement and tremendous support throughout our research work and sharing his technical knowledge has led us through many difficulties easily. This thesis work would have been a difficult task to complete without profiting from his expertise, encouragement and valuable time and criticisms. His endless drive for new and better results is highly appreciated.

We are grateful to Dr. B. D Subudhi, Professor and Head of the Electrical Engineering Department of National Institute of Technology Rourkela, for allowing us to use the necessary facilities for carrying out this thesis work.

We would like to express our heart-felt gratitude to our parents and our family members for being with us when encountering difficulties. Their loving support has been and always will be our most precious possession on earth.

Finally, as it is impossible to mention everybody by name, we would like to convey our thanks to all the teachers and staffs of Electrical Engineering Department and also our friends who have contributed in many ways in making this work a successful one.

Place: National Institute of Technology, Rourkela

Date:

1. A Srikant

2. Shekhar Chandra Pradhan

CONTENTS

Abstract ..... **i**

List of Figures ..... **ii**

List of Tables ..... **iv**

Acronyms and Abbreviations ..... **v**

Chapter 1 Introduction **1**

1.1 Introduction 1

1.2 Objective 2

1.3 Organization of the Thesis 2

Chapter 2 Air Breakdown Mechanism **4**

2.1 Basic Breakdown Process 4

2.1.1. Primary Electrons 4

2.1.2. Ionization 4

2.1.3. Excitation 5

2.1.4. Other Electron Processes 5

2.1.5. Regeneration 5

2.2 Townsend's Mechanism 6

2.2.1. Current Growth Equation 6

2.2.2. Current growth in the presence of secondary process 7

2.2.3. Townsend's criterion for breakdown 8

2.3 Streamer Theory 9

2.3.1. Streamer Theory 9

2.4 Numerical Methods for computation of Electric Field 10

2.4.1 Finite Element Method 11

Chapter 3 Experiment Setup for Air Breakdown Voltage Using Standard Sphere-Sphere Electrode Arrangement **15**

3.1 Apparatus required for measurement of air breakdown voltage 15

3.2 Measurement of Voltage Breakdown of Air 17

3.3 Measurement of Voltage Breakdown of Insulation Paper 18

3.4 SEM analysis of the Insulation Paper 20

Chapter 4 Simulation of Electric Field for Different Electrode Configuration **.....23**
4.1 Simulation of electric field of different electrode arrangements 23
4.1.1 Sphere – Sphere Electrode.....24
4.1.2 Rod-Rod Electrode 27
4.1.3 Rod-Plate Electrode Configuration 29
4.1.4 Comparison of different electrode arrangements 32
Chapter 5 Conclusion **.....33**
References **.....34**

Abstract

Rapid growth in power sector of nation has given the opportunity to power engineers to protect the power equipment for reliable operation during their operating life. It has been seen from the several studies conducted by power engineers that one of the main problem in high voltage power (HV) equipment is the degradation of insulation i.e., quality of insulation of power equipment. As the high voltage power equipments are mainly subjected with spark over voltage causes by the lighting strokes, switching action, a protective device is used for determine the safe clearance required for proper insulation level. The sphere gaps are commonly used for measurements of peak values of high voltages and have been adopted by IEC and IEEE as a calibration device. Generally, the standard sphere gaps are widely used for protective device in electrical power equipments. The sphere gaps are filled up with insulating medium such as liquid insulation (transformer oil), and gas insulation (SF_6, N_2, CO_2, CCl_2F_2 etc.) in HV power equipments. Normally, air medium is widely used as an insulating medium in different electrical power equipments as its breakdown strength is 30kV/cm. Therefore electrical breakdown characteristic of small air gap under the different applied voltage has its great significance for the design consideration of various air insulated HV equipment. In addition, the effect of breakdown voltage on different insulation like lamiflex, leatheroid, plywood, craft paper, and polyester fiber has also been studied. To observe the effect on insulation due to breakdown mechanism, the insulation samples are collected both before and after breakdown voltage test and analysis has been done with the help of Scanning electron microscope (SEM). To simulate the air breakdown voltage with and without the insulation barrier has been studied experimentally in high voltage laboratory, a standard diameter of 25 cm spheres are used for measurement of air breakdown voltages and electric field of the high voltage equipments. The above experiment is conducted at the normal temperature and pressure. The simulation of such air breakdown voltage has been carried out in the COMSOL environment. Finally, the experimental result has been compared with theoretical, and simulation results.

List of Figures

Fig. No.	Name of figure	Page No.
2.1	Arrangement for study of Townsend discharge	6
2.2	Field distortion due to presence of space charge	9
2.3	A typical finite element division of an irregular domain	12
2.4	Typical triangular element; the local node numbering 1-2-3 must proceed counter clockwise as indicated by the arrow	13
3.1	Experimental setup in high voltage test laboratory for study of air breakdown voltage using standard sphere gap method (a) Control panel for conducting the air breakdown test (b) High voltage transformer (c) Two spheres are arranged vertically having 25 cm diameter each	16
3.2	Schematic diagram of the experimental setup	16
3.3	Breakdown voltage vs. gap distance between two spheres	18
3.4	Effect of breakdown voltage on lamiflex paper (a) before breakdown(b) after breakdown	21
3.5	Effect ofbreakdown voltage on Leatheroid paper (a)before breakdown(b)after breakdown	22
3.6	Effect of breakdown voltage on notebook cover (a) before breakdown (b) cover after breakdown	22
4.1	Sphere-sphere electrode (a) electrode arrangement (b) electric field distribution	24
4.2	Maximum electric field (E_{max}) kV/cm vs. gap distance(cm)	25
4.3	Sphere-sphere arrangement with a barrier (a) sphere-sphere arrangement (b) electric field distribution	26

4.4	Comparison of maximum electric field of spheres with and without barrier	26
4.5	Rod-rod analysis without barrier (a) arrangement of rod-rod electrode (b) electric field distribution	27
4.6	Maximum field variation with gap distance	28
4.7	Rod-rod analysis with barrier (a) arrangement of electrodes (b) electric field distribution	28
4.8	Effect of barrier on maximum electric field	29
4.9	Rod-plate analysis without barrier (a) arrangement of rod and plate (b) electric field distribution	30
4.10	Maximum electric field vs. gap distance	30
4.11	Rod-plate analysis with barrier (a) rod-plate arrangement (b) electric field distribution	31
4.12	Maximum electric field vs. gap distance	31
4.13	Comparison of maximum electric field for different electrode arrangements	32

List of tables

Table No.	Table	Page No.
1	Breakdown voltage (V_{bd}) test using sphere – sphere electrode	17
2	Breakdown voltage (V_{bd}) test using different insulators placed in between sphere – sphere electrode	19
3	Photographs of insulation paper before and after breakdown	20

Acronyms and Abbreviations

E_{max}	Maximum electric field
V_{BD}	Breakdown voltage
FEM	Finite element method
SEM	Scanning electron microscope
HV	High voltage
E	Electric field
V	Voltage
ε_r	Relative permittivity
ε_0	Permittivity of free space
D	Electric field displacement

Chapter 1

Introduction

1.1. Introduction

Rapid growth in power sector of nation has given the opportunity to power engineers to protect the power equipment for reliable operation during their operating life. It has been seen from the several studies conducted by power engineers that one of the main problem in high voltage power (HV) equipment is the degradation of insulation i.e., quality of insulation of power equipment [1-7]. As the high voltage power equipments are mainly subjected with spark over voltage causes by the lighting strokes, switching action, a protective device is used for determine the safe clearance required for proper insulation level. The sphere gaps of different configuration are commonly used for this purpose. The sphere gaps are commonly used for measurements of peak values of high voltages and have been adopted by IEC and IEEE as a calibration device. In the past several decades, extensive amount of research work has been done to understand the fundamental characteristics of the electrical breakdown [6-8]. Therefore, electrical breakdown characteristic of small air gap under the different applied voltage has its great significance for the design of overhead line, substation equipment and various air insulated HV equipment. To simulate the air breakdown voltage with and without insulation barrier has been studied experimentally in high voltage laboratory at NIT Rourkela, aluminium made standard spheres of diameter 25 cm is used for measurement of air breakdown voltages and electric field of the high voltage equipments. The above experiment is conducted at the normal temperature and pressure. The simulation of such air breakdown voltage has been carried out in the MATLAB/COMSOL

environment. It helps to determine the insulation needed for the equipment. The simulation helps to evaluate even complex configuration before manufacturing the product. In the following sections are includes experimental setup for air breakdown test in high voltage laboratory, theoretical study, computer simulation and results analysis.

1.2. Objective

The objective is to find the breakdown voltage for sphere- sphere electrode arrangement for different gap distance. Further to simulate the behavior of electric field in different electrode configuration such as sphere-sphere, rod- rod and plate-rod and compare these configurations. These configurations are encountered in most of the designs of high voltage equipments. The knowledge of the field helps to determine the insulation type and their strength to protect the equipment to perform efficiently and avoid failure.

1.3. Organization of the Thesis

The thesis has been organized into five chapters.

Chapter1: It gives introduction about the necessity of breakdown test and how the computer simulation helps in designing the equipments. It gives a brief idea about the objective of the thesis.

Chapter 2: This chapter includes the basic breakdown process and it describes the advantages of numerical methods for calculation of field. The method of finite element has been briefly discussed.

Chapter 3: This chapter includes the experimental set up used and the measurement of breakdown voltage of air and insulation paper using sphere gaps. It also shows how the insulation paper deterioration after breakdown using SEM analysis.

Chapter 4: This chapter includes the simulation of electric field around different configurations (sphere-sphere, rod-rod, and rod-plate). The simulation results with and without barrier have been discussed. Also the comparison of the three configurations has been done.

Chapter 5: In this chapter the breakdown analysis is discussed and the conclusion from SEM results is also discussed. The analysis of different electrode arrangement sphere-sphere, rod-rod, and rod-plate is discussed.

Chapter 2

Air Breakdown Mechanism

2. Air Breakdown Mechanism

Most of the electrical equipments use air as the insulating medium. Various phenomena occur in the air medium when a voltage is applied. When the voltage applied is low, a small currents flow through the air and it retains its electrical properties. On the other hand if the voltage applied is large enough, then the current increases rapidly and an electrical breakdown occurs. A strongly conducting spark is formed, creating a short circuit between the two electrodes. The maximum voltage applied at that moment is called breakdown voltage.

2.1. Basic Breakdown Process

2.1.1. Primary Electrons

Free electrons exist for only short period of time in air that is not subject to high electric field; normally they are trapped, after creation by cosmic radiation to form negative ions. These have a density commonly of the order of a few hundred per cubic centimeter [5].

2.1.2. Ionization

The electrons so liberated can themselves accelerate in the field and collide with neutral molecules and settle down with drift velocity. When they have sufficient energy, the collision may liberate a new electron and a positive ion. The process is cumulative and is quantified by

Townsend and resulting in the formation of avalanches of electrons. The growth in number of electrons and positive ions impart a small conductivity but it is large enough for breakdown [5].

2.1.3. Excitation

Where electrons are sufficiently energetic to cause ionization, there is usually a plentiful supply with lower energies that can excite neutral atoms without liberating electrons. When returning to ground state, these atoms emit visible or ultra violet light. This property is widely used to show the existence of ionization [5].

2.1.4. Other Electron Processes

The electrons created by the growth of ionization may be trapped and so removed from ionisation process. This is the attachment process: a net growth of electron and ion population occurs only when the field is sufficiently high for the rate of ionization to exceed the rate of attachment. Subsequent detachment of electrons from negative ions occurs at the same time, through collisions with neutrals, with free electrons or by interaction with photons. Recombining between electrons and positive ions and between positive and negative ions is a further element in the competing processes that are active in an ionized gas [5].

2.1.5. Regeneration

Initially, Townsend postulated that the positive ions could also ionize, a process now recognized as insignificant. Also that they move towards the negative electrode to release further electrons by secondary emission, so that the ionization process could be sustained and grow indefinitely until breakdown occurred. Experiment later showed that breakdown could occur much more quickly than this process would allow. The solution lay in postulating that he positive ions, created by ionization, are sufficient to create an electric field which, when added to the applied field intensifies the ionization process [5].

2.2. Townsend's Mechanism

2.2.1. Current Growth Equation

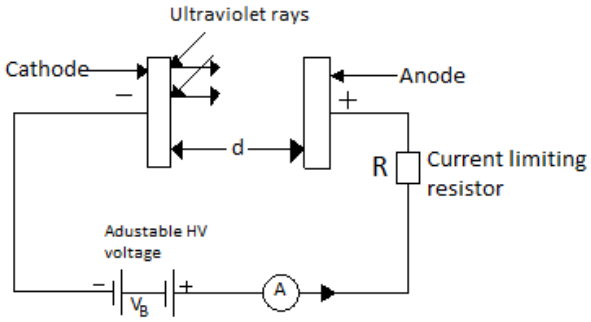

Fig 2.1 Arrangement for study of Townsend discharge

Referring to the Fig. 2.1, let us assume that n_0 electrons are emitted from the cathode. When one electron collides with a neutral particle, a positive ion and an electron are formed. This is called an ionizing collision. Let α be the average number of ionizing collisions made by an electron per centimeter travel in the direction of the field (α depends on gas pressure p and E/p, and is called the Townsend's first ionisation coefficient). At any distance x from the cathode, let the number of electrons be n_x. When these n_x electrons travel a further distance of de they give rise to ($\alpha n_x dx$) electrons [4].

$$\text{At } x=0,\ n_x = n_0$$

$$\text{Also,} \quad \frac{dnx}{dx} = \alpha nx \quad ; \qquad \text{or} \quad n_x = n_0 exp(\alpha x)$$

Then, the number of electrons reaching the anode($x=d$) will be

$$n_d = n_0 \exp(\alpha d) \tag{1}$$

The number of new electrons created, on the average, by each electron is

$$\exp(\alpha d) - 1 = \frac{n_d - n_0}{n_0} \tag{2}$$

Therefore, the average current in the gap, which is equal to the number of electrons travelling per second, will be

$$I = I_0 \exp(\alpha d) \tag{3}$$

Where I_0 is the initial current at the cathode.

2.2.2. Current growth in the presence of secondary process

The single avalanche process described in the previous section becomes complete when the initial set of electrons reaches the anode. However, since the amplification of electrons [exp(αd)] is occurring in the field, the probability of additional new electrons being liberated in the gap by other mechanisms increases, and these new electrons create further avalanches. The other mechanisms are [4]

(i). the positive ions liberated may have sufficient energy to cause liberation of electrons from the cathode when they impinge on it.

(ii). the excited atoms or molecules in avalanches may emit photons, and this will lead to the emission of electrons due to photo-emission.

(iii). the metastable particles may diffuse back causing electron emission.

The electrons produced by this process are called secondary electrons and the coefficient called secondary coefficient Υ i.e. ($\Upsilon = \Upsilon_1 + \Upsilon_2 + \Upsilon_3$) sum of coefficient of individual processes. Following Townsend's procedure for current growth, let us assume

n_0' = number of secondary electrons produced due to secondary (Υ) process

n_0'' = total number of electrons leaving the cathode.

$$n_0'' = n_0 + n_0'$$

The total number of electrons n reaching the anode becomes,

$$n = n_0'' \exp(\alpha d) = (n_0 + n_0')\exp(\alpha d);$$

$$n_0' = \Upsilon\,[\mathrm{n} - (n_0 + n_0')] \tag{4}$$

Eliminating n_0',

$$n = \frac{n_0 \exp(\alpha d)}{1 - \Upsilon\,[\exp(\alpha \mathrm{d}) - 1]} \tag{5}$$

Or,

$$I = \frac{I_0 \exp(\alpha d)}{1 - \Upsilon\,[\exp(\alpha \mathrm{d}) - 1]} \tag{6}$$

2.2.3. Townsend's criterion for breakdown

Equation (6) gives the total average current in a gap before the occurrence of breakdown. As the distance between the electrodes d is increased, the denominator of the equation tends to zero, and at some critical distance $d = d_s$ [4].

$$1 - \Upsilon[\exp(\alpha \mathrm{d}) - 1] = 0 \tag{7}$$

For values of $d<d_s$, I is approximately equal to I_0, and if the external source for the supply of I_0 is removed, I becomes zero. If $d = d_s$, $I \rightarrow \infty$ and the current will be limited by the resistance of the power supply and the external circuit. This is called Townsends's breakdown criterion and can be written as

$$\Upsilon[\exp(\alpha \mathrm{d}) - 1] = 1 \tag{8}$$

Normally, exp(αd) is very large, and hence the above equation reduces to

$$\Upsilon \exp(\alpha d) = 1 \quad (9)$$

For a given gap spacing and at a given pressure the value of the voltage V which gives the values of α and ϒ satisfying the breakdown criterion is called the spark breakdown voltage V_s and the corresponding distance d_s is called the sparking distance.

2.3. Streamer Theory of Breakdown in Air

Townsend mechanism when applied to breakdown at atmospheric pressure is found to have certain drawbacks. Firstly, according to the Townsend theory, current growth occurs as a result of ionisation processes only. But in practice, breakdown voltages were found to depend on the gas pressure and the geometry of gap and electrodes. Secondly, the mechanism predicts time lags of the order of 10^{-5} s, while in actual practice breakdown is observed to occur at very short time of the order of 10^{-10} s. the Townsend mechanism failed to explain the observed phenomena and Streamer theory is proposed [4].

2.3.1. Streamer Theory

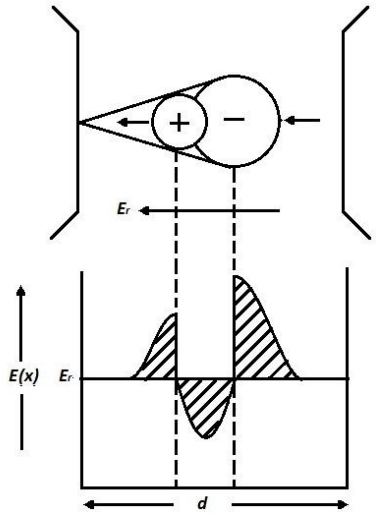

Fig 2.2 Field distortion due to presence of space charge

Fig. 2.2 shows the electric field around the avalanche as it progresses along the gap and the resulting modification to the applied field. For simplicity, the space charge at the head of the avalanche is assumed to have a spherical volume containing negative charge at its top because of the higher electron mobility. Under these conditions, the field gets enhanced at the top of the avalanche with field lines from the anodes terminating on its head. Further, at the bottom of the avalanche, the field between electrons and ions reduces the applied field (E). Still further down, the field between cathode and the positive ions gets enhanced. Thus, the field distortion occurs and it becomes noticeable with a charge carrier number $n > 10^6$. If a charge density in the avalanche approaches $n = 10^8$ the space charge filled field and the applied field will have the same magnitude and this leads to the streamer. Thus space charge fields play an important role in the growth of avalanches in corona and spark discharges in non-uniform field gap.

2.4. Numerical Methods for computation of electric field

In recent years, several numerical methods for solving partial differential equations which include Laplace's and Poisson's equations have become available. There are inherent difficulties in solving these equations for two or three dimensional fields with complex boundary conditions, or for insulating materials with different permittivities and/or conductivities [4].

Proper design of any high voltage apparatus requires a complete knowledge of the electric field distribution. For a simple physical system with some symmetry, it is possible to find an analytical solution. However, in many cases, the physical systems are very complex and therefore in such cases, numerical methods are employed for the calculation of electric fields. Essentially, three types of numerical methods are commonly employed in high voltage engineering applications. They are: Finite Element method (FEM), Charge Simulation Method (CSM), and Surface Charge Simulation Method (SSM) or Boundary Element method (BEM)

Here, we have used Finite Element method.

2.4.1 Finite Element Method

Finite Element Method is widely used in the numerical solution of electric field problems. In contrast to other numerical methods, FEM is a very general method and therefore is a versatile tool for solving wide range of electric field problems [4, 10-12].

The finite element analysis of any problem involves basically four steps:

(a). Finite Element Discretization

To start with, the whole domain is fictitiously divided into small areas/volumes called elements (see Fig.2.3). The potential, which is unknown throughout the problem domain, is approximated in each of these elements in terms of the potential at their vertices called nodes. As a result of this the potential function will be unknown only at the nodes. Normally, a certain class of polynomial is used for interpolation of the potential inside each element in terms of their nodal values. The coefficient of this interpolation function is then expressed in terms of the unknown nodal potentials. As a result of this, the interpolation can be directly carried out in terms of the nodal values. The associated algebraic functions are called shape functions. The elements derive their names through their shape, i.e. bar elements in one dimension (1D), triangular and quadrilateral elements in 2D, and tetrahedron and hexahedron elements for 3D problems [4,11].

(b). Governing Equations

The potential V_e within an element is first approximated and then interrelated to the potential distributions in various elements such that the potential is continuous across inter-element boundaries. The approximate solution for the whole region then becomes [10-12]

$$V(x,y) = \sum_{e=1}^{N} V_e(x,y) \tag{10}$$

Where N is the number of elements into which the solution region is divided.

The most common form of approximation for the voltage V within an element is a polynomial approximation

$$V_e(x,y) = a + bx + cy \tag{11}$$

For the triangular element and for the quadrilateral element the equation becomes

$$V_e(x,y) = a + bx + cy + dz \tag{12}$$

The potential V_e in general is not zero within the element *e* but it is zero outside the element in view of the fact that the quadrilateral elements are non-confirming elements (see Fig.2.3).

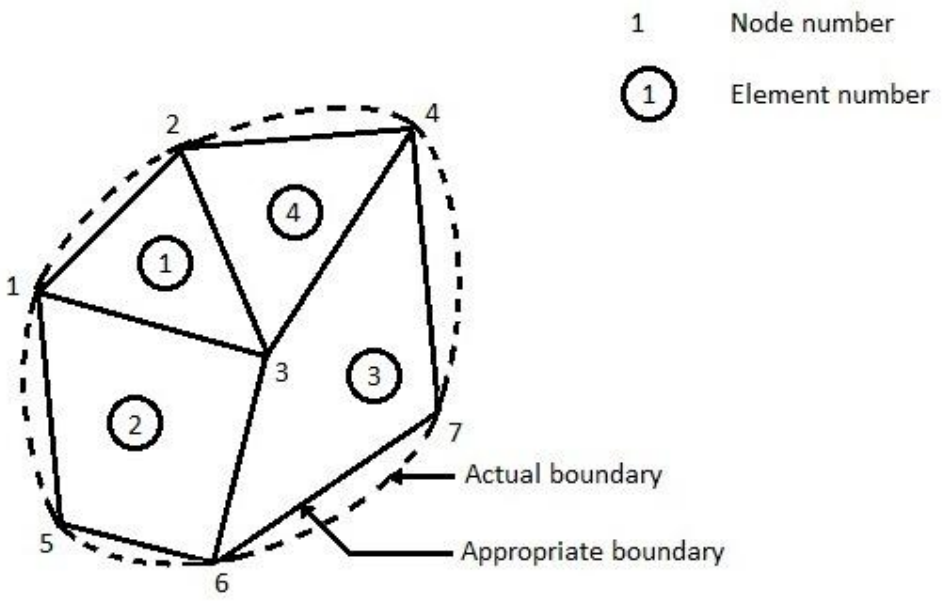

Fig. 2.3 A typical finite element division of an irregular domain

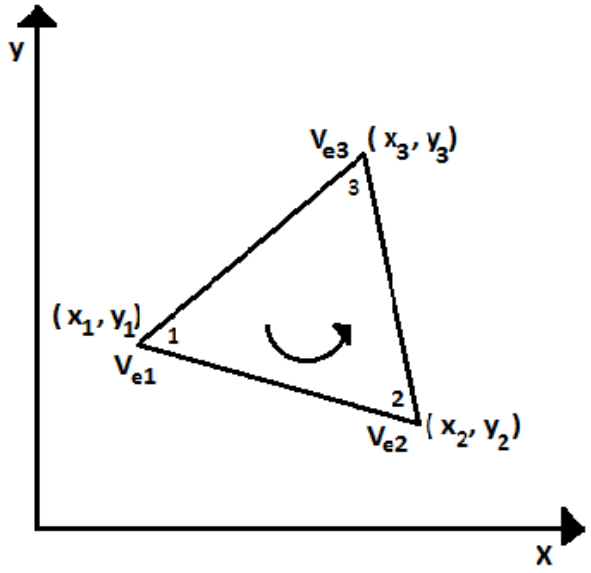

Fig. 2.4 Typical triangular element; the local node numbering 1-2-3 must proceed counterclockwise as indicated by the arrow

Consider a typical triangular element shown in Fig. 2.4., the potentials V_{e1}, V_{e2} and V_{e3}at nodes 1, 2, and 3 are obtained from Eq. (11), as

$$\begin{bmatrix} V_{e1} \\ V_{e2} \\ V_{e3} \end{bmatrix} = \begin{bmatrix} 1 & x_1 & y_1 \\ 1 & x_2 & y_2 \\ 1 & x_3 & y_3 \end{bmatrix} \begin{bmatrix} a \\ b \\ c \end{bmatrix} \tag{13}$$

The coefficients a, b, and c are determined from the above the above equation as

$$\begin{bmatrix} a \\ b \\ c \end{bmatrix} = \begin{bmatrix} 1 & x_1 & y_1 \\ 1 & x_2 & y_2 \\ 1 & x_3 & y_3 \end{bmatrix}^{-1} \begin{bmatrix} V_{e1} \\ V_{e2} \\ V_{e3} \end{bmatrix} \tag{14}$$

Substituting this equation in Eq. (12), we get

$$V_e = [1 \quad x \quad y]\ 1/2A \tag{15}$$

$$\begin{bmatrix} x_2y_2 - x_3y_2 & x_3y_1 - x_1y_3 & x_1y_2 - x_2y_1 \\ y_2 - y_3 & y_3 - y_1 & y_1 - y_2 \\ x_3 - x_2 & x_1 - x_3 & x_2 - x_1 \end{bmatrix} \begin{bmatrix} V_{e1} \\ V_{e2} \\ V_{e3} \end{bmatrix} \tag{16}$$

Or,

$$V_e = \sum_{i=1}^{N} \alpha_{i(x,y)} V_{ei} \tag{17}$$

The energy per unit length associated with the element e is given by the following equation:

$$W_e = 1/2\varepsilon[V_e]^T[C^{(e)}][V_e] \tag{18}$$

Where, T denotes the transpose of the matrix

$$[V_e] = \begin{bmatrix} V_{e1} \\ V_{e2} \\ V_{e3} \end{bmatrix} \tag{19}$$

and

$$[C^{(e)}] = \begin{bmatrix} C_{11}^{(e)} & C_{12}^{(e)} & C_{13}^{(e)} \\ C_{21}^{(e)} & C_{22}^{(e)} & C_{23}^{(e)} \\ C_{31}^{(e)} & C_{32}^{(e)} & C_{33}^{(e)} \end{bmatrix} \tag{20}$$

(c) Assembling of All Elements

Having considered a typical element, the next stage is to assemble all such elements in the solution region. The energy associated with all the elements will then be

$$W_e = \sum_{e=1}^{N} W_e = 1/2\varepsilon[V]^T[C][V] \tag{21}$$

(d) Solving the resulting equations

The resulting equations are solved to find the necessary quantities at different nodes.

Chapter 3

Experiment Setup for Air Breakdown Voltage Using Standard Sphere-Sphere Electrode Arrangement

3.1. Experimental Setup for measurement of air breakdown voltage

To conduct the air breakdown test between the sphere electrode all the measuring instrument is standardized as per IS 2071. Figure 3.2 shows the schematic diagram of experimental setup. In this study two identical sphere electrodes have been used for the experimental study of the short air gap. The sphere electrodes are vertically aligned. The lower sphere electrode which is above the ground plane is grounded where as the top sphere electrode is connected with HV connector. The used sphere electrode has a diameter of 25 cm and the electrode is made of Aluminum material with nickel coating and air is acting as an insulating medium between sphere electrodes. Before conducting the test the two sphere electrodes are cleaned with carbon tetra chloride (CCl_4) so that it is free from floating dust particles, fibers. The upper sphere electrode is connected in the high voltage terminal and the lower electrode is connected with the ground terminal. With the application of the high voltage between the sphere electrodes, a non-uniform electric field is generated as the surfaces of the sphere electrodes are not uniform. The HV electrode is energized from the 50 Hz transformer with a power rating of 15kVA with a transformation ratio of 230V/100kV. The applied voltage is raised to 75% of the estimated voltage and thereafter the voltage is raised 2% of the test voltage per second [6-8, 13]. The test voltages are applied through the filter unit to isolate the noise of the transformer from the measuring circuit and current limiting device for protect in case of complete breakdown and

prevent the high frequency current to the high voltage lead. At the inception of the breakdown the circuit is immediately disconnected from the supply and the breakdown voltage is recorded. A coupling device with connecting cable is associated with the measuring circuit for the measurement of the applied high voltages magnitude. The experimental setup for air breakdown study between the two spheres electrode are shown in Fig. 3.1.

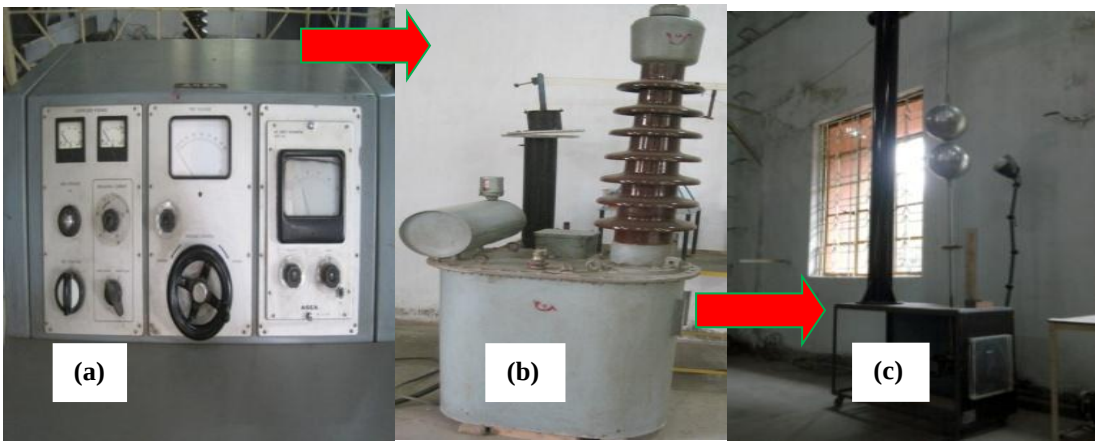

Fig. 3.1 Experimental setup in high voltage test laboratory for study of air breakdown voltage using standard sphere gap method (a) Control panel for conducting the air breakdown test (b) High voltage transformer (c) Two spheres are arranged vertically having 25 cm diameter each.

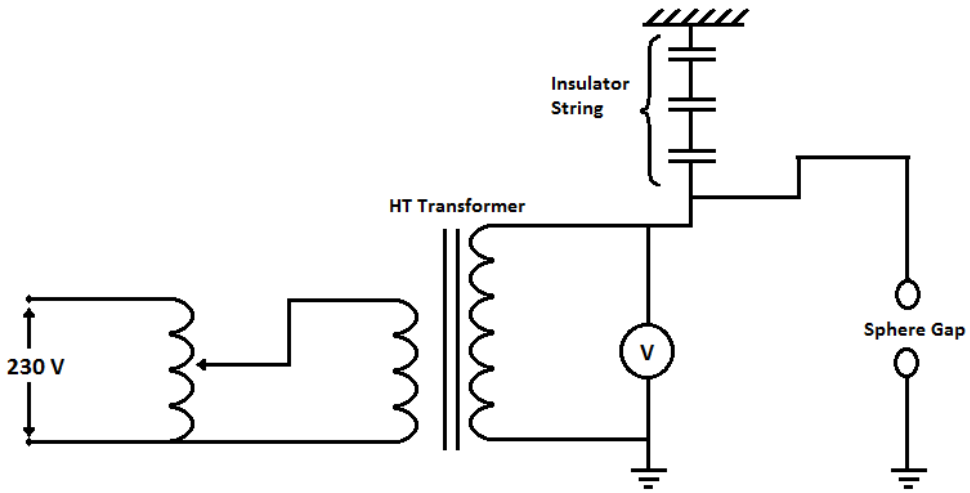

Fig. 3.2 Schematic diagram of the experimental setup

3.2. Measurement of Voltage Breakdown of Air

The experiment is conducted at High Voltage Engineering Lab, NIT Rourkela. The experiment is conducted for Sphere-Sphere Electrode. The diameter of the sphere is 25cm and is made of aluminium. For different spacing between the two spheres, the breakdown voltage is observed [13-14].

TABLE I

BREAKDOWN VOLTAGE (V_{BD}) TEST USING SPHERE – SPHERE ELECTRODE

Air gap distance (cm)	Rms value of Breakdown voltage (kV)	Peak value of Breakdown voltage (kV) ($V_{BD,peak}$)	Peak Breakdown voltage with correction = k*$V_{BD,peak}$
0.5	7.8	11.03	11.13
1	19.5	27.58	27.82
1.5	30.5	43.13	43.51
2	39.5	55.86	56.35
2.5	50	70.71	71.33
3	59.5	84.14	84.88
3.5	66.5	94.05	94.88
4	80	113.14	114.14
4.5	86	121.62	122.69
5	95.5	135.06	136.25

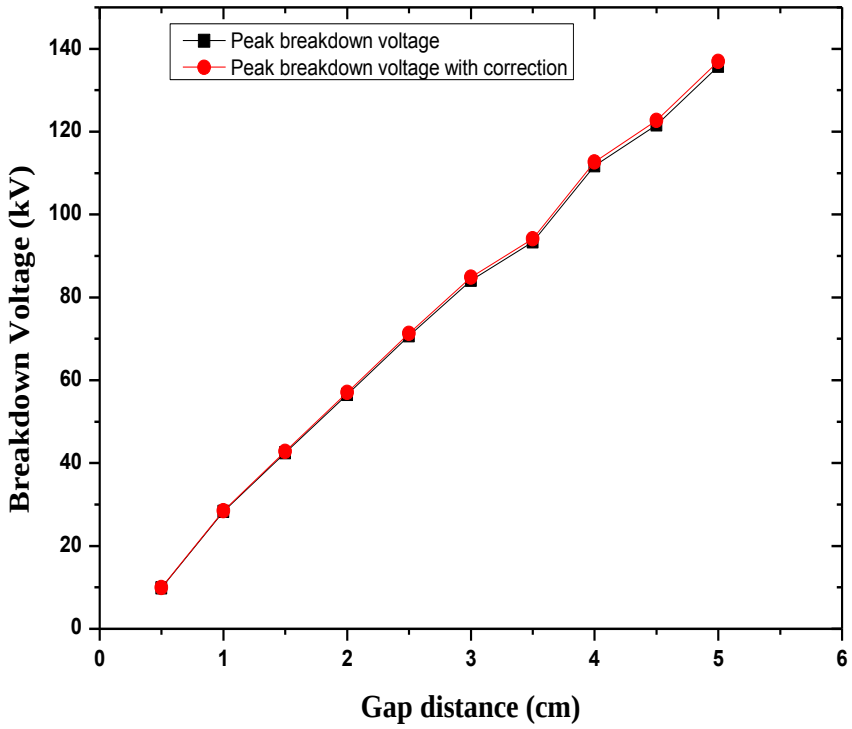

Fig. 3.3 Breakdown voltage vs. gap distance between two spheres

3.3. Measurement of Voltage Breakdown of Insulation Paper

Again, the experiment is conducted having insulator between the two spheres and the breakdown voltages for different insulation materials is observed. The breakdown strength of the polyester fiber is the highest followed by lamiflex, leatheroid, craft paper, paper and plywood which is depicted in Table 2.

TABLE II
BREAKDOWN VOLTAGE (V_{BD}) TEST USING DIFFERENT INSULATORS PLACED IN BETWEEN SPHERE – SPHERE ELECTRODE

Insulation Material	Thickness (mm)	Breakdown Voltage (kV)
Paper	0.26	6.68
	0.52	6.85
	1.04	7.21
Ply wood	1.9	3.58
Polyester fibre	1.62	41.35
Lamiflex	0.22	3.5
	0.44	9.8
Leatheroid	0.19	3.2
	0.38	7.0
Craft paper	0.22	15
	0.44	23.5

TABLE III

PHOTOGRAPHS OF INSULATION PAPER BEFORE AND AFTER BREAKDOWN

Insulating Material	Thickness (mm)	Photograph of insulation before Breakdown Voltage test	Photograph of insulation after Breakdown Voltage test
Paper	0.26		
	0.52		
	1.04		
Ply wood	1.9		

3.4. Scanning Electron Microscope Test

A Scanning Electron Microscope (SEM) is a type of electron microscope that images a sample by scanning it with a high-energy beam of electrons in a raster scan pattern. The electrons interact with the atoms that make up the sample producing signals that contain information about the sample's surface topography, composition, and other properties such as electrical conductivity. The types of signals produced by an SEM include secondary electrons, back-scattered electrons (BSE), characteristic X-rays, light (cathodoluminescence), specimen current and transmitted electrons. Secondary electron detectors are common in all SEMs, but it is rare that a single machine would have detectors for all possible signals. The signals result from interactions of the electron beam with atoms at or near the surface of the sample. In the most

common or standard detection mode, secondary electron imaging or SEI, the SEM can produce very high-resolution images of a sample surface, revealing details about less than 1 to 5 nm in size. Due to the very narrow electron beam, SEM micrographs have a large depth of field yielding a characteristic three-dimensional appearance useful for understanding the surface structure of a sample

The SEM test is conducted at SEM Laboratory, NIT Rourkela using JEOL-JSM-6480LV SEM instrument. The SEM photographs are shown below. The Figures 3.4, 3.5 and 3.6 show how the insulation paper gets deteriorated after the breakdown of the papers.

1. Lamiflex Paper

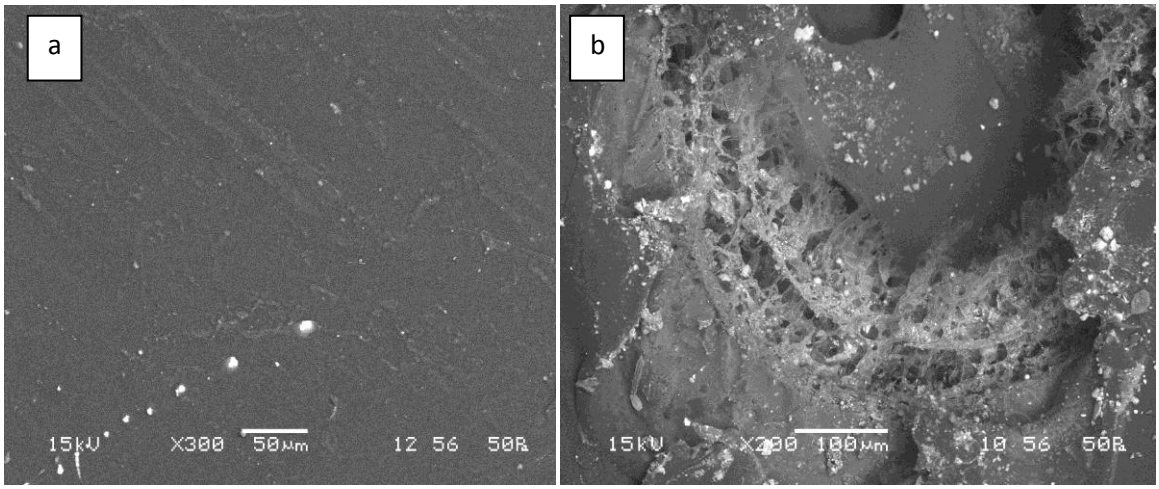

Fig 3.4 Effect of breakdown voltage on lamiflex paper (a) before breakdown (b) after breakdown

2. Leatheroid Paper

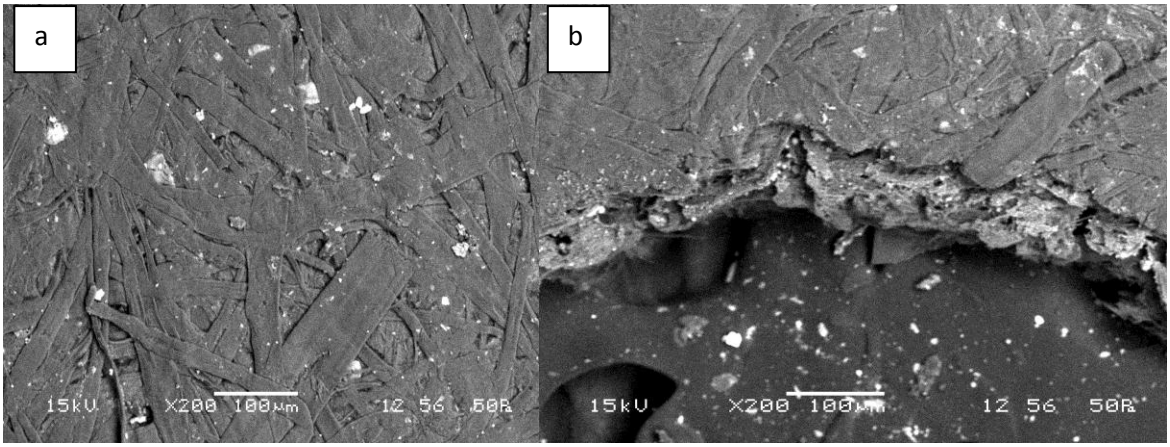

Fig. 3.5 Effect ofbreakdown voltage on Leatheroid paper (a) before breakdown (b) after breakdown

3. Notebook Cover

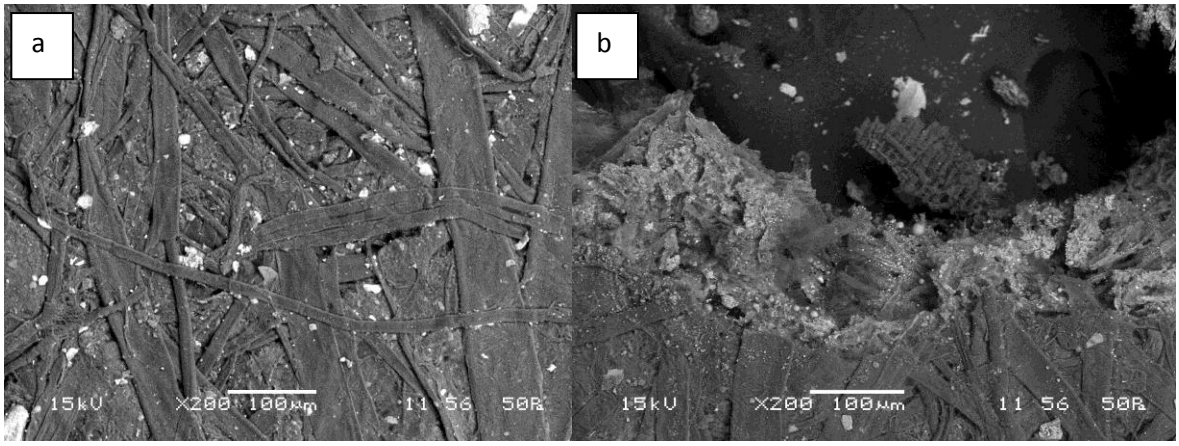

Fig. 3.6 Effect of breakdown voltage on notebook cover (a) before breakdown (b) cover after breakdown

From the Table 2 and Figures 3.5, 3.6, 3.7 it is observed that the Lamiflex paper has the highest breakdown voltage and from SEM photographs also it is shown that it is least deteriorated. So, if Lamiflex paper among the above tested insulation paper is used for insulation, the high voltage equipment protection will be efficient.

Chapter 4

Simulation of Electric Field for Different Electrode Configuration

4.1. Simulation of electric field of different electrode arrangements

The simulation of electric fields in three different configuration is observed using COMSOL Multi-physics software [15]. In electrostatics, Maxwell's equations and constitutive equation reduce to the following form

$$\nabla \times E = 0 \tag{22}$$

$$\nabla \cdot D = \rho \tag{23}$$

$$D = \varepsilon E \tag{24}$$

where E is the electric field intensity, D is the electric displacement, ρ is the space charge density, ε is the dielectric permittivity of the material. Based on Eq. (1), electric field intensity is introduced by the negative gradient of the electric scalar potential V in following form

$$E = -\nabla V \tag{25}$$

Substituting equations (2) and (3) in (1) Poisson's scalar equation is obtained as

$$-\nabla \cdot (\varepsilon \nabla V) = -\nabla \cdot (\varepsilon_0 \varepsilon_r \nabla V) = \rho \tag{26}$$

where ε_0 is the permittivity of free space, $\varepsilon_r = \varepsilon_r(E, x, y, z)$ is the relative permittivity and ρ is the space charge density. If the permittivity ε is constant such as in the isotropic dielectrics, Eq. (26) becomes

$$\Delta V = -\rho\, \varepsilon \tag{27}$$

For space charge free ($\rho = 0$) fields, field is expressed by Laplace's equation as $\Delta V = 0$.

In this study, solution of the problem is obtained from solution of Laplace's equation in rectangular coordinates.

$$\nabla^2 V = \frac{\partial^2 V}{\partial^2 x} + \frac{\partial^2 V}{\partial^2 y} + \frac{\partial^2 V}{\partial^2 z} \tag{28}$$

V = Breakdown voltage on the upper electrode,

V = 0 Volt (ground) on the lower electrode,

$\partial V/\partial n = 0$ on all other outer boundaries and on the symmetry axis and $n.(D_1 - D_2) = 0$ on the surfaces of the dielectric barrier as continuity condition. The electrodes are made of aluminium and are surrounded by air. The barrier used is Poly Vinyl Chloride (PVC).

4.1.1 Sphere – Sphere Electrode

Firstly, the electric field between two spheres arrangement (see Fig. 4.1(a)) is observed. The radius of the sphere is12.5 cm and the gap distance is varied between the two spheres, and the maximum electric field (E_{max}) for the applied voltage is observed.

(a). Without Barrier

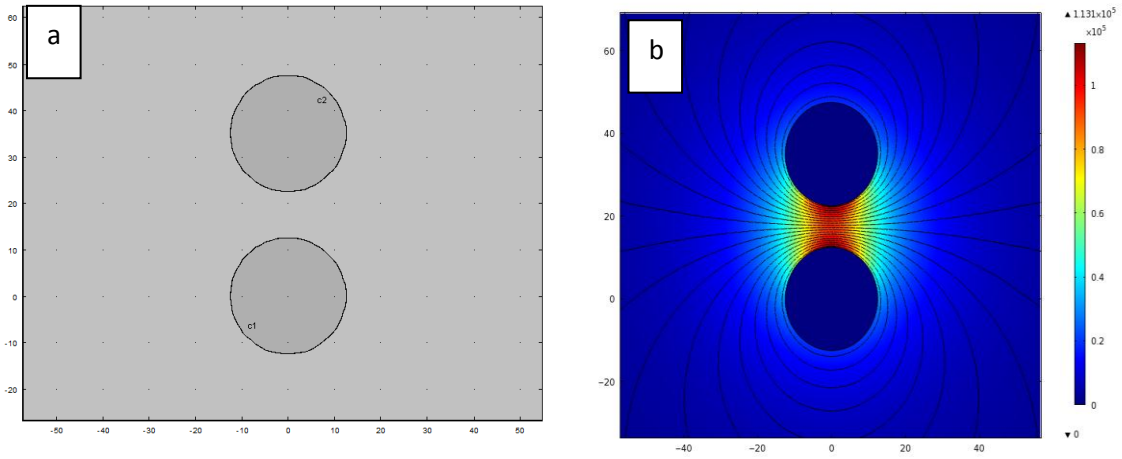

Fig. 4.1 Sphere-Sphere Electrode (a) Electrode arrangement (b) Electric Field Distribution

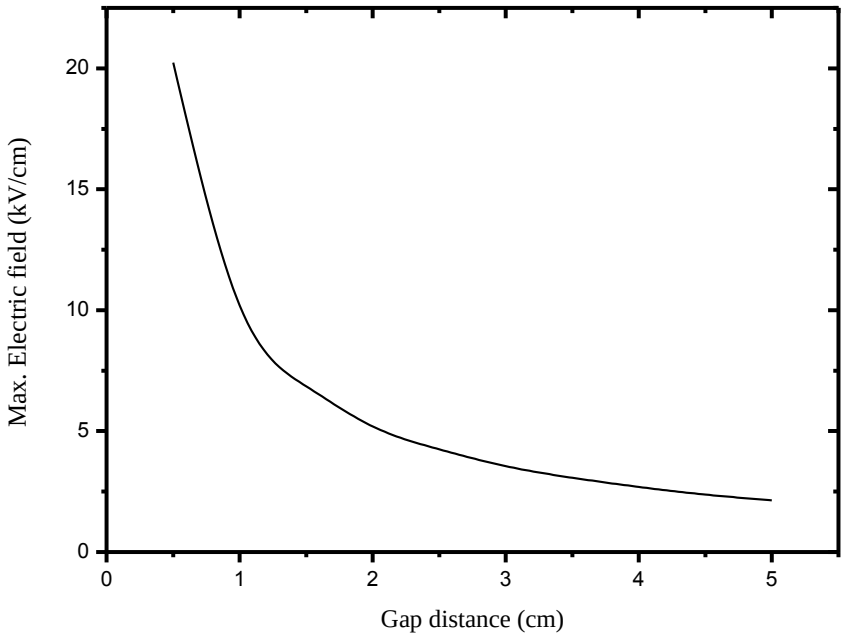

Fig. 4.2 Maximum electric field (E_{max}) kV/cm vs. gap distance (cm)

From Fig. 4.1 it is observed that the electric field distribution is non- uniform for sphere-sphere electrode arrangement. The electric field is non-uniform about the y- axis. Figure 4.2 shows that the maximum electric field decreases with the increase in the gap distance. In the beginning there is sharp drop in the maximum electric field but it gradually saturates with increase in the gap distance.

(b). Effect of the Barrier

To observe the effect of barrier, a barrier made of PVC (of ε = 2.9) thickness 0.25cm is introduced and the electric field distribution is observed. Figure 4.1 (a) shows the arrangement of the sphere electrodes. The electrodes are made of aluminum and they are surrounded by air. Fig. 4.1(b) shows the electric field distribution for this arrangement. The electric field is observed to be non-uniform.

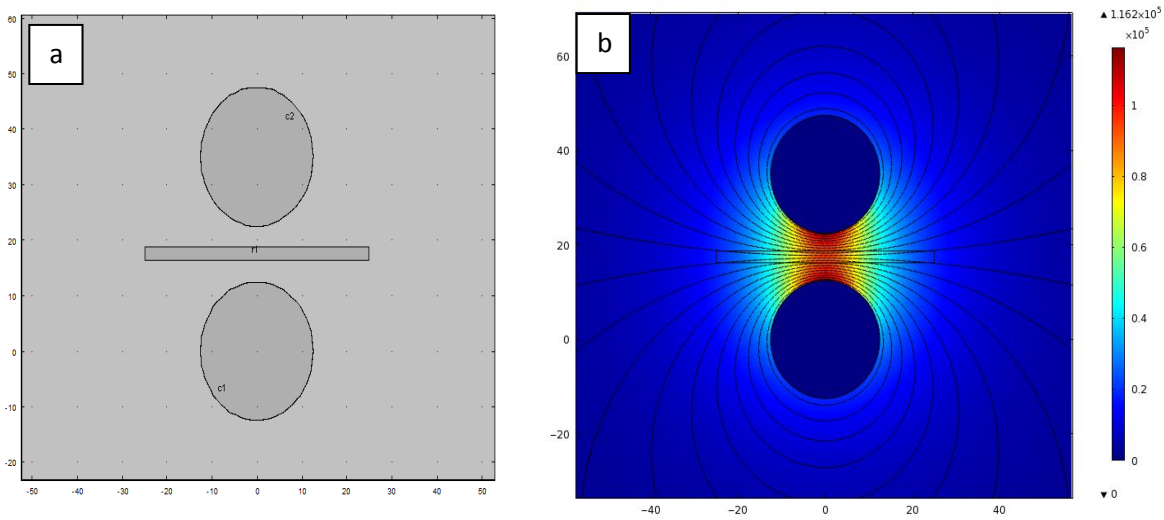

Fig. 4.3 Sphere-Sphere arrangement with a barrier (a) sphere-sphere arrangement (b) electric field distribution

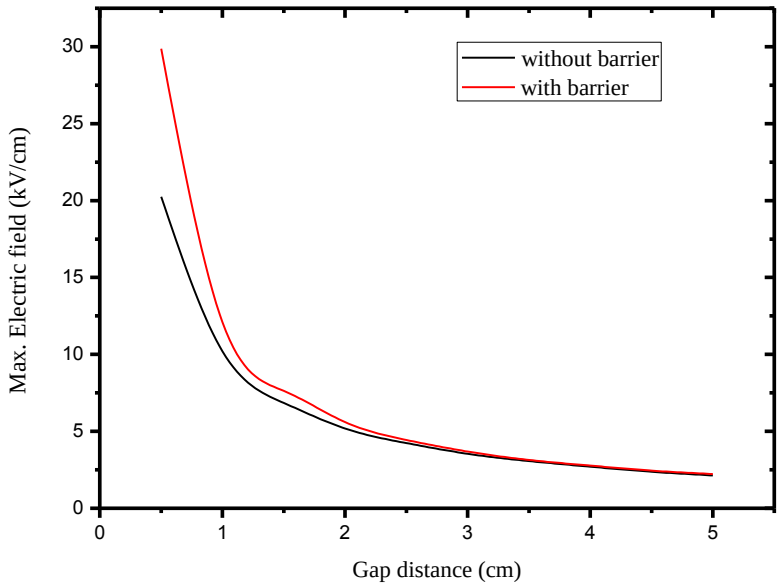

Fig. 4.4 Comparision of maximum electric field of spheres with and without barrier.

In Fig. 4.4, the comparision between the maximum electric field with and without barrier has been shown. It shows that maximum electric field (E_{max}) for arrangement with barrier is more than Emax for the electrode arrangement without barrier.

4.1.2 Rod-Rod Electrode

Firstly, the electric field distribution for rod-rod electrode arrangement without a barrier is observed, then a barrier of PVC (ε = 2.9) is introduced to observe the effect on electric field.

(a) Without Barrier

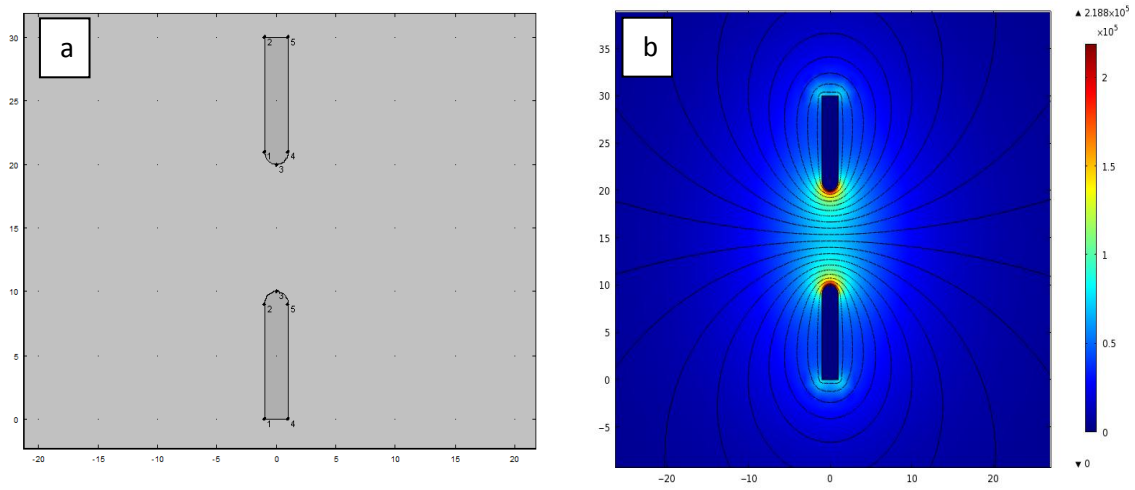

Fig. 4.5 Rod-rod analysis without barrier (a) arrangement of rod-rod electrode (b) electric field distribution

The Fig. 4.5(b) shows that the electric field distribution is non-uniform for rod – rod arrangement and the electric field is symmetric about the y-axis. The electric field is maximum at the tip of the rod and it decreases along the axis joining the rods and again increases. The electric field between the rods is much more inhomogeneous than in the sphere-sphere arrangement.

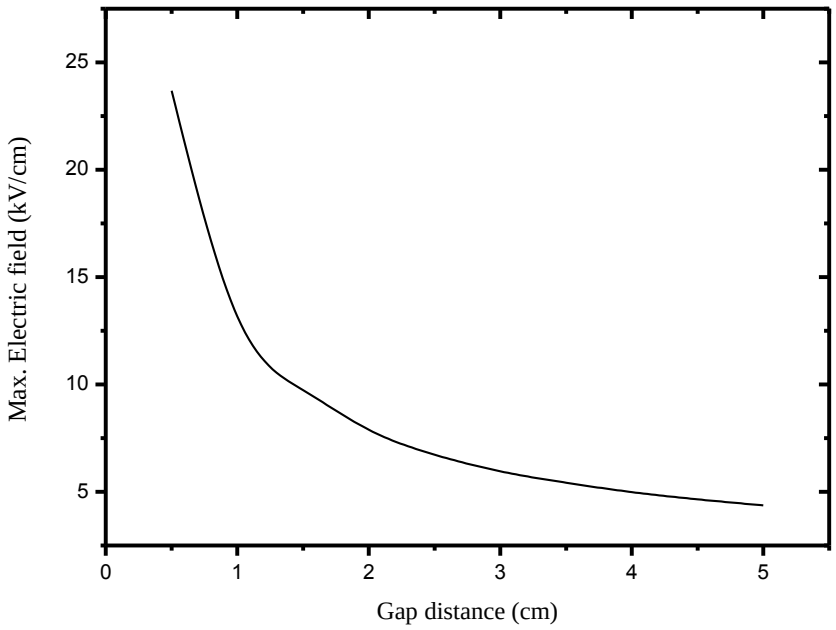

Fig. 4.6 Maximum field variation with gap distance

(b) Effect of Barrier

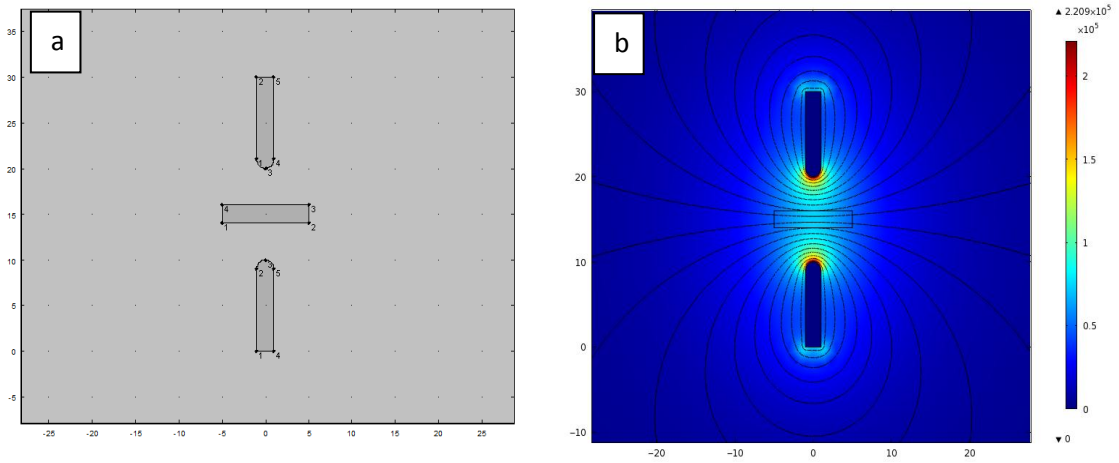

Fig. 4.7 Rod-rod analysis with barrier (a) arrangement of electrodes (b) electric field distribution

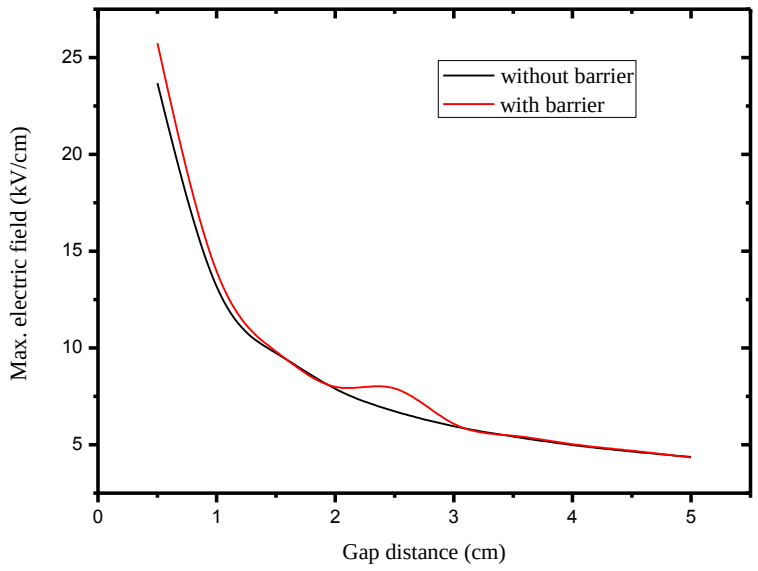

Fig.4.8 Effect of barrier on maximum electric field

Fig. 4.5 (b) and Fig. 4.7 (b) shows that the electric field distribution between two rods is non-uniform and is symmetric about the y-axis. Fig. 4.6 shows the variation of Emax with gap distance. Fig. 4.8 shows how the maximum electric changes with introduction of barrier.

4.1.3 Rod-Plate Electrode Configuration

To observe the field distribution in rod plate arrangement with and without barrier the arrangments as shown in Fig. 4.9 (a) and Fig. 4.11 (a) are made. The electrodes are made of aluminium and are surrounded by air. The length of rod is 10cm and the width is 1 cm . The diameter of the plate is 10cm and the thickness is 1 cm. The barrier used is made of PVC (ε = 2.9). By varying the gap distance between the rod and plate the electric field distribution and the maximum electric field values were noted and plotted against gap distance. The electric field observed in rod plate gap is non-uniform in nature.

(a) Without Barrier

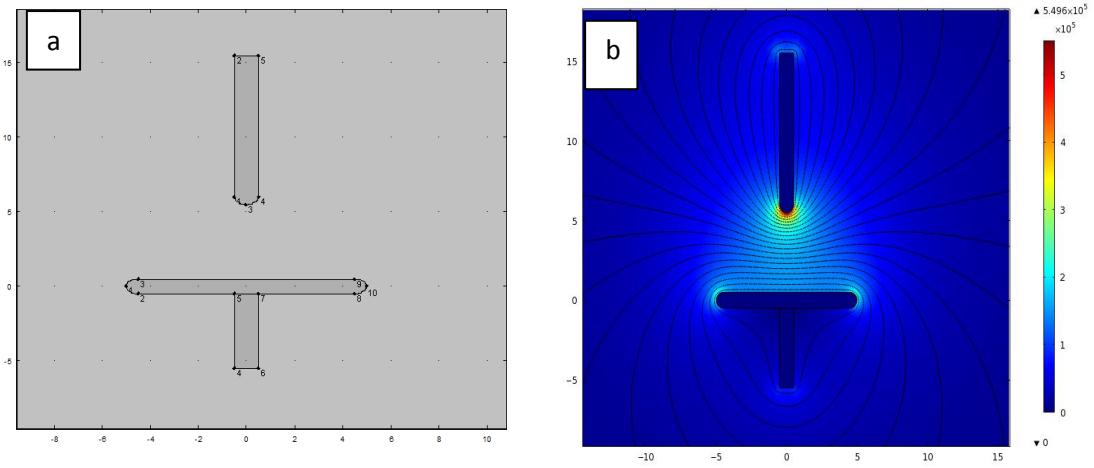

Fig. 4.9 Rod-plate analysis without barrier (a) arrangement of rod and plate (b) electric field distribution

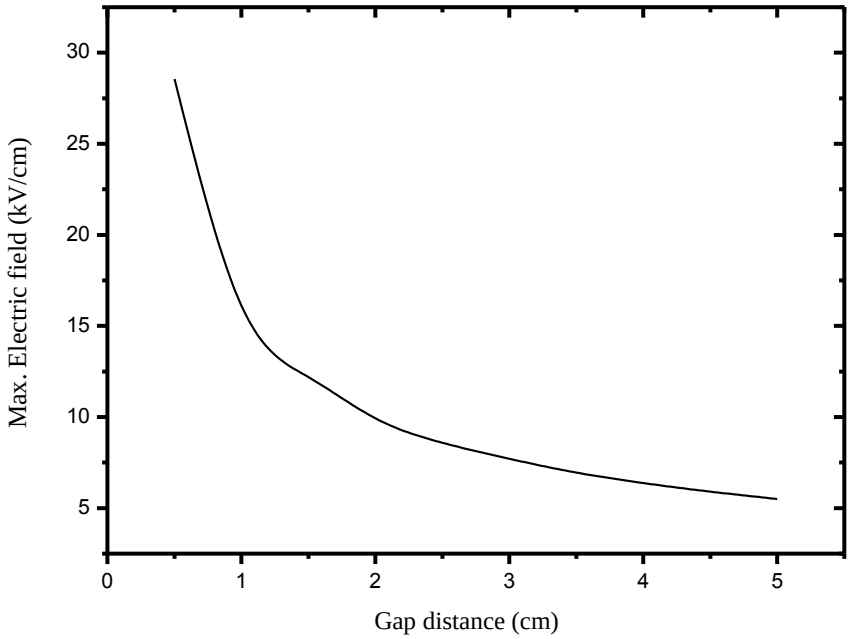

Fig. 4.10 Maximum electric field vs. gap distance

(b). Effect of Barrier

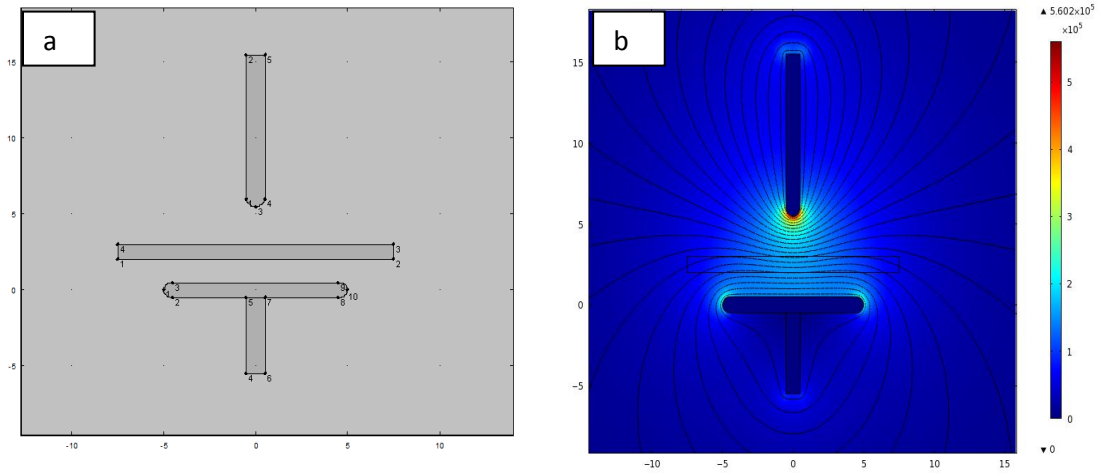

Fig. 4.11 Rod-plate analysis with barrier (a) rod-plate arrangement (b) electric field distribution

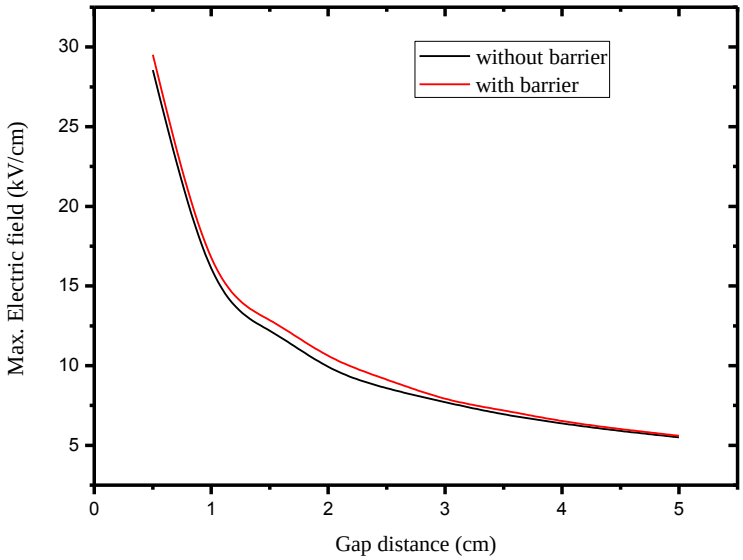

Fig. 4.12 Maximum electric field vs. gap distance

Fig. 4.9 (b) and Fig. 4.11 (b) shows that the electric field distribution in the rod plate gap is non uniform in nature. Figure 4.12 shows the comparision of maximum electric field with and without barrier.

4.1.4 Comparison of different electrode arrangements

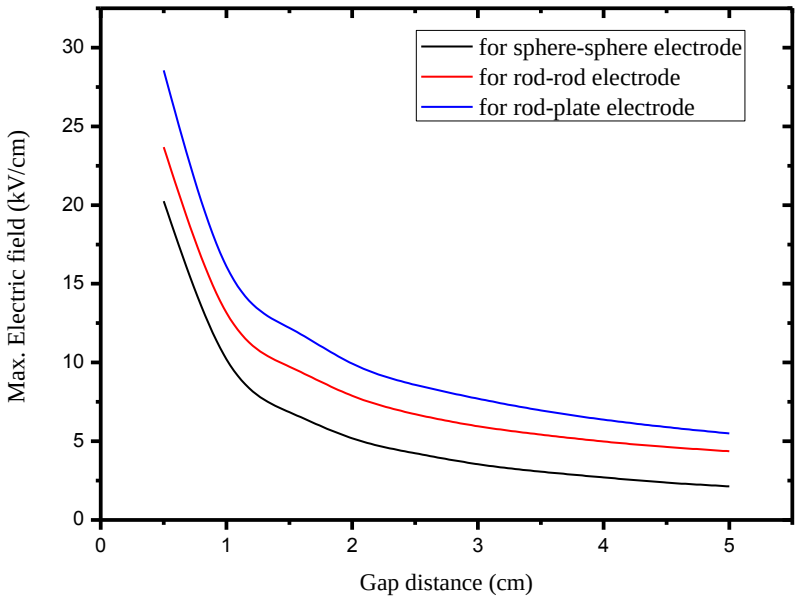

Fig. 4.13 Comparison of maximum electric field for different electrode arrangements

Fig. 4.13 shows the comparision between the three electrode arrangements. It is observed from the graph that the plate-rod electrode arrangement has the highest value of E_{max} followed by rod-rod and sphere-sphere.. From Fig. 4.5 (b) and 4.7 (b) however, the rod-rod air gap is a symmetric arrangement, the electric field is much more inhomogeneous than the sphere- sphere arrangement. From Fig. 4.9 (b) and 4.11 (b) it is shown that, the rod-plate arrangement is non symmetric arrangement in nature. The electric field between the electrodes is more inhomgeneous than other arrangements.

Chapter 5

Conclusion

In this study the breakdown mechansim has been investigated with help of sphere-sphere electrode both experimentally and by simulation with COMSOL environment. It has been studied from the result in both cases that the maximum electric field intensity not only changes with the geometrical confguration of electrodes but also changes with other parameters like distance between the electrode, applied voltage between the electrode as well as temperature and pressure. However, both the experimental and simulation results has been done in this study considering no change of physical condition like temperature and pressure. From the breakdown test, it is observed that the breakdown voltage increases with increase in gap distance between the two electrodes. In addition, the effect of breakdown voltage on different insulation like lamiflex, leatheroid, plywood,craft paper, and polyster fibre has also been studied. To observe the effect on insulation due to breakdown mechansim, the insulation samples are collected both before and after breakdown voltage test and analysis has been done with the help of Scanning electron microscope (SEM). The SEM analysis showed the level of detoriation in three different insulation papers. It is observed from the SEM analysis that the detoriation of such insulation is minimum for lamiflex paper. In case of breakdown phenomena observed bysimulation study with the help of COMSOL in different electrode arrangements like sphere-sphere, rod-rod and rod-plate. The above study conclude that electric field distribution for rod-rod or rod-plate in air medium is strongly affected by the geometry (shape and dimensions) of electrodes and the distance between electrodes. The distribution of electric field is more inhomogenous in rod-plate

than the rod-rod and sphere- sphere gap. The maximum value of the electric field strength along the axis of the gap at breakdown voltage tends to get a steady value in case of symmetric arrangements such as sphere- sphere, rod-rod etc. but in unsymmetric arrangement like rod-plate, the maximum value of field strength increases with gap length.

The test electrodes are kept in air medium without considering temperature and pressure of air. So in future the simulation can be done introducing the pressure and temperature parameters. The simulation can be done for complex configuration like transmission tower, circuit breaker, transformer, bushing, high voltage reactors etc.

References

[1] S. Pillai and R. Hackam "Electric field and potential distributions for unequal spheres using symmetric and asymmetric applied voltages" *IEEE Transactions on Electrical Insulation,* Vol. EI-18, No.5, October 1983.

[2] E. Kuffel, W. S. Zeangle & J. Kuffel, '*High Voltage Engineering Fundamentals'*, published by Butterworth-Heinemann 2nd edition, 2000.

[3] N. K. Kishore, G. S. Punekar, H. S. Y. Shastry, "Spark over in sphere gaps with alternating voltages and perturbed electric fields", annual report conference on '*Electrical Insulation and Dielectric Phenomena*', 2009.

[4] M.S. Naidu and V. Kamaraju, '*High Voltage Engineering'*, published by Tata McGraw-Hill 3rd edition, 2004.

[5] A Haddad and D. Warne "Advances in High Voltage Engineering", published by IET 1st edition,2004.

[6] J. H. Colete and J. V. Merwe "The breakdown electric field between two conducting spheres by the method of images" *IEEE trans on education*, Vol.41,No.2,May 1998.

[7] Y. Nishikori, S. Kojima, and T. Kouno "A study of the field utilization factor and the maximum electric field at spark over of the standard sphere gaps" *Translated from Denki Gakkai Ronbunshi*, Vol.21-B, No.3, March 2001.

[8] S. Phontusa and S. Chotigo "The proposed humidity correction factor of positive dc breakdown voltage of sphere-sphere gap at h/δ lower than 13 g/m³" *2nd IEEE International Conference on Power and Energy (PECon 08),* , Johor Baharu, Malaysia, December 1-3, 2008.

[9] J. B. Nah. kang, Y. D. Chung, M. C. Ahn, D. K. Bae and T. K. Ko "Study on the breakdown voltage characterization of insulation gases for devoleping a high voltage superconducting apparatus" IEEE Transactions on Applied Superconductivity, Vol.20, No.3, June 2010.

[10] Matthew N. 0. Sadiku "A Simple introduction finite element analysis of electromagnetic problems", IEEE transactions on education, vol. 32, no. 2, may 1989.

[11] O.W. Andersen "Finite element solution of complex potential electric fields" IEEE Transactions on Paver Apparatus and Systems, Vol. PAS-96, no. 4, July/August 1977.

[12] James F. Hoburg "A student-oriented finite element program for electrostatic potential problems" IEEE transactions on education, vol. e-26, no. 4, november 1983.

[13] A. Pedresen "Calculation of spark breakdown or corona starting voltages in nonuniform fields" IEEE transactions on power apparatus and systems vol. pas-86, no. 2 february, 1967.

[14] M. Mahdy, H. I. Anis and S. A. Ward "Electrode Roughness Effects on the Breakdown of Air-insulated Apparatus" IEEE Transactions on Dielectrics and Electrical Insulation Vol. 5 No. 4, August 1998.

[15] A Kara, Ö. Kalenderli, K. Mardikyan "Effect of dielectric barriers to the electric field of rod-plane air gap"Excerpt from the Proceedings of the COMSOL Users Conference 2006 Prague.